scientific reports

OPEN

Predicting thermal and electromagnetic performance of omndirectional magnetic field generators via figure of merit

Mason Pratt, Tim Ameel & Sameer R. Rao✉

Omnidirectional magnetic field generators, or Omnimagnets, are electromagnetic devices used for non-contact manipulation tasks. Supplying current to an Omnimagnet generates a magnetic field and generates Joule heating, which can cause overheating. Omnimagnets are thermally limited. Omnimagnet design currently relies on advanced thermal-electromagnetic simulations, which can vary widely between applications. Currently, there is no generalized understanding for coupled thermal-electromagnetic effects. This work addresses this knowledge gap by developing a universal framework for estimating Omnimagnet performance directly from the design and operating conditions. Scaling analysis is used to determine the coupling between thermal and electromagnetic effects in terms of design variables and base principles. The scaling relationships are used to define a figure of merit η where a higher η indicates a superior design. Equations are fitted to simulated Omnimagnet performance for multiple cooling mechanisms (convection, radiation) and different electromagnetic priorities (dipole moment *m*, *m*/mass). Quantitative relationships are developed that can predict Omnimagnet performance across a spectrum of designs without requiring advanced thermal and electromagnetic simulations (i.e. $m = 530\eta_{conv}$ for convectively-cooled Omnimagnets, where $\eta_{conv} = h^{0.5}(T_{max} - T_{\infty})^{0.5}L_{max}^{3.5}$ is the figure of merit). The figure of merit η can also be used to gauge Omnimagnet performance for new applications, as is shown for power-sensitive Omnimagnets. Using this methodology, non-experts can use a figure of merit to streamline the design of Omnimagnets for new or existing use cases. The methodology is broadly applicable for the design of similar electromagnetic devices such as electrical motors, generators, and electromagnets.

Keywords Thermal design, Omnimagnet, Scaling analysis, Thermal management, Electromagnetic analysis, Space debris remediation

If space debris is not actively removed from Earth orbits, humankind risks losing access to space itself. Collisions between objects in orbit can lead to Kessler Syndrome[1] and the proliferation of space debris, preventing satellite deployment and space travel. Omnidirectional magnetic field generators, or Omnimagnets, have recently gained attention as a potential solution for non-contact space debris removal[2–4]. Omnimagnets are novel electromagnetic devices that remotely manipulate non-magnetic, electrically-conductive objects using eddy currents[5]. Omnimagnets have primarily found use in biomedical[6–8] and aerospace[2–4] applications where non-contact manipulation is desirable. An Omnimagnet's electromagnetic strength is fundamentally coupled with its thermal performance due to the onset of overheating[5]. Large voltages and currents are required to power these devices, generating considerable Joule heating. The concentric geometry of Omnimagnets thermally insulates the innermost components and leads to elevated local temperatures. All of these effects limit the current that can be safely supplied to an Omnimagnet, decreasing its magnetic strength. Improving the design of Omnimagnets to increase heat dissipation and reduce heat generation will delay the onset of overheating failure and thus increase electromagnetic performance.

The links between Omnimagnet performance and thermal effects, electromagnetic strength, and design parameters are not well understood[9–11]. Further, the definition of Omnimagnet performance is highly dependent on application: Omnimagnets used in biomedical applications are designed to generate very powerful magnetic fields over small amounts of time[7] whereas aerospace applications focus on long-term magnetic field strength

Department of Mechanical Engineering, University of Utah, Salt Lake City, UT 84112, USA. ✉email: s.rao@utah.edu

per mass[10] due to mass limitations of rocket payloads. The different constraints of each application have been investigated separately, but it remains unclear how to design the best Omnimagnets for new applications and new sets of constraints. Convective cooling has been the preferred method of thermal management for biomedical applications. Transient lumped-capacitance thermal analysis was employed to predict Omnimagnet overheating for convectively-cooled Omnimagnets[11,12]. Other cooling methods, such as phase-change materials and internal convective cooling of the frames, have also been investigated[11]. It was shown that increasing the size of the Omnimagnet is thermally beneficial and increases the time before overheating occurs. These modeling efforts report quantitative thermal improvements but fail to directly relate the thermal and magnetic effects. The fundamental relationship between the thermal and magnetic behavior of convectively-cooled Omnimagnets remains unknown. Omnimagnets for aerospace applications are designed to operate at a quasi-steady-state condition in Earth orbits. Radiative cooling is the primary mode of heat rejection for these applications. Thermal resistance networks[10,13] and finite-element analysis[9] have been used to study the thermal behavior of radiatively-cooled Omnimagnets. Effects of discrete design changes have been investigated, such as additional radiators[13], scaling of Omnimagnet size[9], and optimal ferromagnetic core size[10]. The reported results are discrete observations of a coupled thermal-electromagnetic relationship, but prior work falls short of quantifying the nature of this relationship. Even more, it is unclear how to merge findings from convectively- and radiatively-cooled Omnimagnets. Separate work has demonstrated thermal advantages for increasing Omnimagnet size, but it is unclear if this benefit is tied to the same physics, or if all Omnimagnets should be as large as possible in all applications. It is very difficult to develop a general Omnimagnet design philosophy using focused, specific results.

The task of optimizing an electromagnet is difficult because system performance and constraints are highly contextual. Magnetic field strength, mass, electrical power requirements, volume, and thermal performance can all be key parameters for different applications. Previous electromagnet optimization work tends to focus on only one or two of these parameters, thus limiting the value of the findings to one specific application. Cylindrical electromagnets and solenoids are the simplest and most studied geometry. The maximum magnetic field per electromagnet volume has been identified for cylindrical electromagnets[14]. The cylindrical electromagnet geometry was related to the electromagnetic strength, but mass and thermal limitations were not considered. The optimal cylindrical geometry has been demonstrated to maximize electromagnetic strength for a constant power input by relating field strength H to Joule heating via the supplied current[15]. Thermal contributions from Joule heating were considered, but the impact of different cooling mechanisms was not investigated. The magnetic field strength has been maximized specifically for cylindrical electromagnets cooled via integrated thermally conductive cold discs[16]. The presence of the cold discs inhibits magnetic field generation but simultaneously improves cooling, allowing an increased current to be supplied. However, the findings cannot be generalized to deduce how conductive cold discs could be used for another geometry, or how other cooling mechanisms may compare for the same geometry. For mass-constrained applications, cylindrical electromagnet mass was reduced by 70% for only a 10% increase in supplied electrical power[17]. Recent work has used coupled thermal and electromagnetic models to better understand the design of electrical machines, such as electric motors and generators[18,19]. Scaling analysis has been used to make recommendations for the size[20] and torque-speed curves[21] of electric vehicle motors. Cooling of induction motors was improved via thermal analysis[22] and lithium-ion battery monitoring was accomplished using a coupled electrochemical-magnetic-thermal model[23]. Prior research has clearly improved electromagnet design principles, but it is difficult to combine individual contributions and develop a holistic understanding of electromagnet design for different applications.

There exists a need to improve the Omnimagnet design process by studying the relationships between thermal effects, electromagnetic effects, and common design parameters. Current approaches use advanced modeling to investigate very specific applications, which cannot be synthesized into an understanding of general Omnimagnet operation or design. A highly generalized and adaptable approach is necessary to capture application-driven differences such as alternative cooling mechanisms, mass constraints, and power requirements. To address this knowledge gap, this work develops a universal framework to estimate the performance of an Omnimagnet, regardless of application, by defining a figure of merit to capture key Omnimagnet design and performance variables. This approach calculates Omnimagnet performance from base principles and can be adjusted to account for different applications, cooling mechanisms, and more, which prior work has never accomplished. One coupling equation is developed to link Omnimagnet thermal effects, electromagnetic strength, and design parameters via supplied current density J. This framework is then used to develop guidelines for Omnimagnet design for a variety of applications. Despite differences in cooling mechanism and electromagnetic quantities of interest across Omnimagnet applications, the fundamental thermal-electromagnetic coupling remains constant and can be utilized for many general applications. Using this general coupling, the impact of Omnimagnet length L_{max}, maximum temperature before overheating T_{max}, convective heat transfer coefficient h, and cooling fluid temperature T_∞ are investigated on m produced by convectively-cooled Omnimagnets using a previously published coupled thermal-electromagnetic (T-EM) model[10]. The effect of each variable is combined into a convective figure of merit, η_{conv}, which estimates m produced by a given convectively-cooled Omnimagnet. Increasing an Omnimagent design η_{conv} will generally increase m as well. Using η_{conv} allows researchers and even non-experts to estimate the performance of a convectively-cooled Omnimagnet using simple, fundamental equations rather than advanced modeling techniques. This process is repeated for radiatively-cooled Omnimagnets: the effects of L_{max}, T_{max}, frame emissivity ε_F and solenoid emissivity ε_S are measured on m/mass of the Omnimagnet, which is a key performance metric for space-bound Omnimagnets. A figure of merit, η_{rad}, is formulated using the scaling of each individual design parameter. Finally, the framework is then applied to a new Omnimagnet application that has never been explored before, maximizing m per power input for a radiatively-cooled Omnimagnet. A figure of merit, η_{power}, is easily formulated that can inform researchers how best to design an Omnimagnet for this new application. The coupled thermal-electromagnetic relationship shown here is widely applicable to any thermally-limited Omnimagnet. Comparisons can be rapidly made between different design directions, and even directly compare different cooling mechanisms, without the need for advanced simulations. This work represents a step forward not only in the theoretical understanding of Omnimagnet operation but also in the practical implementation of Omnimagnets for real-world manipulation tasks. This process may be applicable to permanent magnet electrical machines, such as motors, which are similar devices that also experience coupled thermal-electromagnetic behavior and are limited by overheating.

Methodology
Omnimagnet design and operation
An Omnimagnet is formed by surrounding a ferromagnetic core with three orthogonal, concentric solenoids (Fig. 1). Supplying the solenoids with current generates a magnetic field. Each solenoid can be independently supplied with current to precisely control the magnitude and direction of the generated magnetic field. Aluminum frames are used to rigidly support the solenoids. Solenoids and frames are numbered starting from the center of the Omnimagnet and moving outward. The axial lengths of solenoids 1, 2, and 3 are defined as L_1, L_2, and L_3, respectively. The side length of the ferromagnetic core is denoted L_c.

The coupled relationship of interest is between Omnimagnet thermal and electromagnetic effects. Intuitively, the supplied current lies at the center of the link between thermal and electromagnetic effects. Both the amount of heat generated via Joule heating, q_{Joule}, and magnetic dipole moment, *m*, depend on the supplied current. Magnetic dipole moment *m* is conventionally used to measure the magnetic strength of an Omnimagnet[5,10]. The thermal limitations of the device place constraints on the current, which then limits the electromagnetic strength of the device. The quantitative scaling of this coupled relationship is obtained by evaluating current using both thermal and magnetic equations. Then, the two expressions can be set equal to determine a quantitative coupling equation for thermal and magnetic effects.

Omnimagnet thermal scaling analysis
Heat is generated via Joule heating whenever a current is supplied to a solenoid. Joule heating is calculated using Joule's Law[24]: $q_{Joule} = I^2 R$, where *q* is the heat generation rate, *I* is current, and *R* is electrical resistance. Omnimagnets are conventionally designed by specifying a current density *J* rather than current *I*, which are related by the wire cross-sectional area, $I = JA_{wire}$. Current density *J* does not change with wire gauge, simplifying the geometric design variables of an Omnimagnet. The total heat generation of an Omnimagnet thus expressed as

$$q_{Joule} \propto J^2 R \tag{1}$$

Electrical resistance *R* of a solenoid is dependent on the material resistivity and the size and shape of the solenoid. Changing the resistivity is not of interest for this work, as copper solenoids already have very low resistivity relative to other materials. Previous analysis[5] demonstrated that $R \propto L_{max}^3$, where L_{max} is the maximum dimension of an Omnimagnet (i.e., size of a minimum bounding cube). This approximation holds for all Omnimagnets with square cross-section solenoids, which is the most common Omnimagnet geometry. Substituting this expression into Eq. (1) and rearranging to solve for *J* gives an expression for current density in terms of thermal quantities:

$$J \propto q_{Joule}^{0.5} L_{max}^{-1.5} \tag{2}$$

Omnimagnet electromagnetic scaling analysis
Omnimagnet strength is conventionally evaluated using the magnetic dipole moment *m* due to the dipole-like fields that are generated[5,10]. The magnetic dipole moment produced by one square solenoid surrounding a cubic ferromagnetic core is[10]

$$m_i = J_i \left[\frac{6}{\pi} L_i L_c^3 \int_{\beta_{i,1}}^{\beta_{i,2}} \arctan\left(\frac{1}{\sqrt{1+2\zeta^2}} \right) d\zeta + \frac{L_i^4}{6} \left(\beta_{i,2}^3 - \beta_{i,1}^3 \right) \right] \tag{3}$$

where *m* is the dipole moment, *J* is the supplied current density, *L* is the axial length of a solenoid, L_c is the length of the cubic ferromagnetic core, β_1 and β_2 are aspect ratios, and ζ is an arbitrary integration variable. Figure 1 demonstrates how these variables relate to Omnimagnet geometry. The subscript *i* indicates a specific solenoid, i.e. m_1, J_1, and L_1 correspond to solenoid 1. Rearranging Eq. (3) to solve for *J* is trivial, but this would represent *J* in terms of very abstract quantities. To help clarify the magnetic effect in terms of tangible design inputs, scaling arguments are used to simplify Eq. (3) into a more tractable form. Equation (3) shows that magnetic dipole moment is calculated by multiplying *J* by two terms: the first integral term represents the field produced by a magnetized cubic core. The second L_i^4 term represents the field produced by the powered solenoid. These terms will be referred to as the core component and solenoid magnetic component, respectively.

First, the order of magnitude of the core component and solenoid component are compared to determine if any terms are negligible. The core and solenoid components are multiplied by constants $6/\pi$ and 1/6, respectively. The aspect ratios β_1 and β_2 also generate constants. Omnimagnet geometry is defined such that β_1 and β_2 are limited to small ranges: $0 \leq \beta_1 \leq 1$ and $1.291 \geq \beta_2 \geq 1$[5]. Across this range of values, the integral term of the core component in Eq. (3) is a constant between 0 and 0.8166. Likewise, the difference of cubed aspect ratios in the solenoid component takes a value between 0 and 2.15. Multiplying these geometry-defined constants by the appropriate constants $6/\pi$ and 1/6 yields ranges of 0–1.56 and 0–0.36, respectively. These constants have the

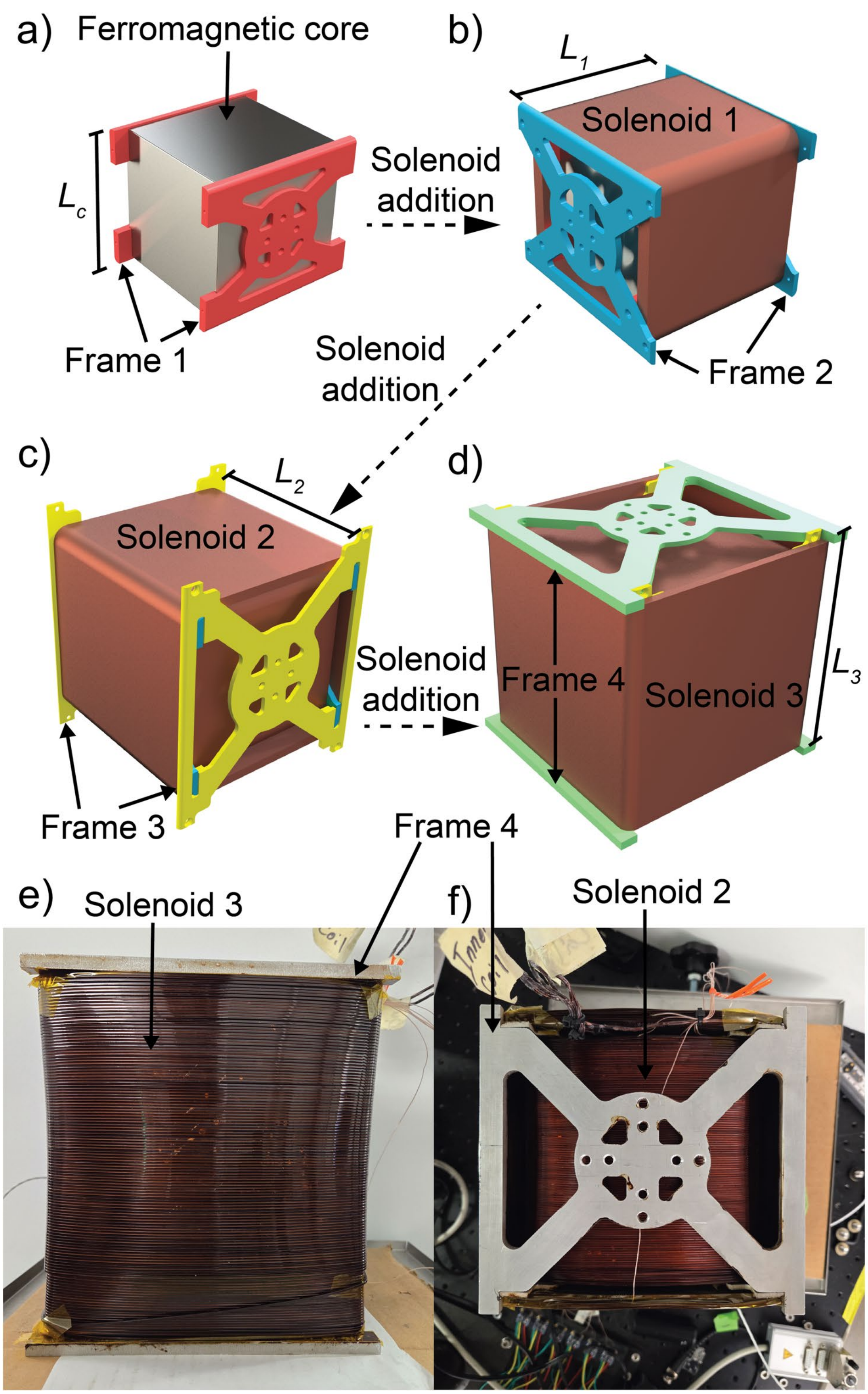

Fig. 1. Omnimagnet geometry schematic. (**a**–**d**) Concentric layers of the Omnimagnet, starting from the innermost layer and moving radially outward. (**e**) Side-view photograph of Omnimagnet. (**f**) Top-view photograph of Omnimagnet.

same order of magnitude and thus show that both the core and solenoid components are important to consider for a scaling analysis. After eliminating the constant terms, the dipole moment can be approximated using

$$m_i \propto J_i(L_i L_c^3 + L_i^4) \tag{4}$$

The various lengths in Eq. (4) can be simplified further. By definition, the length of solenoid 3 is equal to the length of one side of the Omnimagnet, $L_3 = L_{max}$. The length of the core must also be equal to the length of solenoid 1, $L_c = L_1$. For Omnimagnet geometries with reasonably large ferromagnetic cores (i.e. $L_c/L_{max} \geq 0.1$), the lengths of the core, the Omnimagnet, and all three solenoids will be on the same order of magnitude, and all can be represented by a single length *L*. Previous work demonstrated that well-designed Omnimagnets utilize ferromagnetic cores in the range $0.4 \leq L_c/L_{max} \leq 0.8$[10]. For geometries in this range, it is guaranteed that the lengths of the core, solenoid, and overall dimensions will be on the same order of magnitude. Thus, the dipole moment can be simplified to $m_i \propto J_i L_{max}^4$. Current densities supplied to the solenoids are either identical[5] or very similar[9,10], and all current densities can be represented by a general current density *J*. The scaling arguments suggest that the magnetic dipole moment of all three solenoids can be expressed as:

$$m \propto J L_{max}^4 \tag{5}$$

This expression agrees with previous Omnimagnet research on the length scaling of Omnimagnets[9]. Rearranging to solve for *J* defines the current density as a function of electromagnetic quantities:

$$J \propto m L_{max}^{-4} \tag{6}$$

Omnimagnet coupled thermal-electromagnetic relationship

Substituting Eq. (2) into Eq. (6) yields the relationship between Omnimagnet thermal and electromagnetic effects:

$$m L_{max}^{-4} \propto q_{Joule}^{0.5} L_{max}^{-1.5} \tag{7}$$

For clarity, this expression is rearranged to directly relate *m* to Omnimagnet design variables and thermal effects:

$$m \propto q_{Joule}^{0.5} L^{2.5} \tag{8}$$

This expression captures the fundamental relationship between Omnimagnet strength via dipole moment *m* and the heat generation q_{Joule}. The form of Eq. (8) is confirmed via the Buckingham-π theorem in the Supplementary Information. Critically, steady-state conditions require that Joule heating is equal to the heat rejected from the device, $q_{Joule} = q_{out}$. This equality means that *m* produced by an Omnimagnet is directly related to the mechanism of heat rejection, such as convection or radiation. Modeling convectively-cooled Omnimagnets can be accomplished using $q_{out} = hA(T - T_\infty)$, where *h* is the convective heat transfer coefficient, *A* is the surface area of convection, *T* is the Omnimagnet surface temperature, and T_∞ is the working fluid temperature[25]. Radiatively-cooled Omnimagnets can be investigated with Eq. (8) using $q_{out} = \varepsilon\sigma A(T^4 - T_\infty^4)$, where ε is the average emissivity and σ is the Stefan–Boltzmann constant[26]. This approach can be extended to any Omnimagnet application where q_{out} can be attributed to a specific thermal management strategy. Importantly, very few assumptions were made to reach Eq. (8); Relevant Omnimagnets must use square cross-section solenoids (which help to maximize the solenoid packing density[5]), must be roughly cubic (L_{max} can define geometry in *x*-, *y*-, and *z*-directions), must use relatively large ferromagnetic cores ($L_c/L_{max} \leq 0.1$), and must operate at steady-state. To the authors' knowledge, every Omnimagnet that has been manufactured meets the first three criteria.

Results and discussion

Convectively-cooled omnimagnet scaling

Equation (8) captures the thermal and electromagnetic tradeoff that exists during Omnimagnet operation with very few assumptions. While prior experiments and coupled models are inherently limited in scope to specific operating modes and cooling mechanisms, Eq. (8) can be used not only to easily model a wide variety of Omnimagnet systems but also draw important conclusions from the results. The relation between thermal and electromagnetic effects in Eq. (8) is verified using an existing coupled thermal-electromagnetic (T-EM) model[10]. This model calculates the temperature distribution and resulting dipole moment *m* for any Omnimagnet geometry, any operating condition, and any supplied current. The generated *m* calculated by the T-EM model is compared to the estimate from Eq. (8) for verification. Notably, the T-EM model does not assume any of the scaling relations discussed in this work. The T-EM model rigorously considers the electromagnetic and thermal effects during Omnimagnet operation. The estimates via Eq. (8) can be calculated two to three orders of magnitude faster than the T-EM model.

Omnimagnets cooled via convection are typically designed to produce the maximum possible dipole moment *m*. It follows that the relationship between *m* and thermal and geometric parameters should be investigated to inform Omnimagnet design and maximize *m*. For an Omnimagnet that rejects heat using only convection to an ambient temperature T_∞, heat rejection can be represented as $q_{conv} = hA_s(T_{max} - T_\infty)$, where *h* is the prescribed heat transfer coefficient on the exposed surfaces of solenoid 2, solenoid 3, and frame 4, A_s is the convective surface area of those same components, T_{max} is the maximum safe temperature before overheating

Parameter	Minimum	Reference	Maximum
L_{max} [m]	0.025	0.172	0.6
T_{max} [K]	273	473	673
T_{∞} [K]	253	293	363
h [W/m^2·K]	5	250	5000

Table 1. Parametric variable ranges for convectively-cooled omnimagnet.

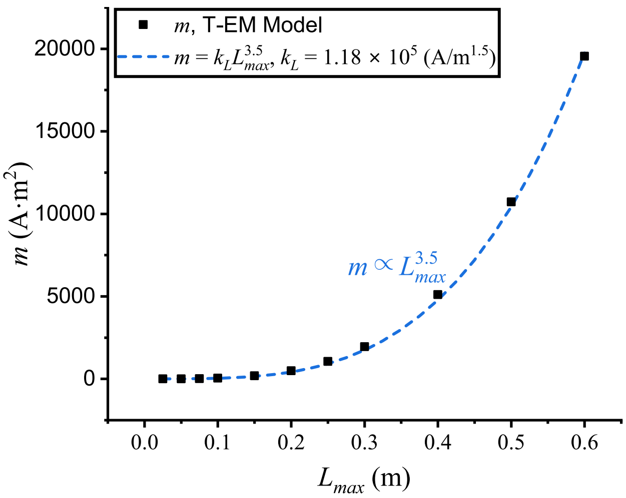

Fig. 2. Verification of predicted expression $m \propto L_{max}^{3.5}$ for a convectively-cooled Omnimagnet. The expression closely matches the T-EM model results for 11 Omnimagnets ($r^2 = 0.999$). Small increases of L_{max} dramatically increase *m* produced by an Omnimagnet.

failure occurs, and T_{∞} is the cooling fluid temperature[25]. By recognizing the convective area A_s is $A_s \propto L_{max}^2$ for the roughly cube-shaped Omnimagnet, Eq. (8) becomes

$$m_{conv} \propto h^{0.5}(T - T_{\infty})^{0.5} L_{max}^{3.5} \tag{9}$$

The T-EM model is used to evaluate *m* while L_{max}, T_{max}, T_{∞}, and *h* are parametrically varied. The minimum, reference, and maximum values are detailed in Table 1. The reference values of *h*, T_{max}, and T_{∞} are based on prior Omnimagnet convective cooling analysis[11]. The reference value of L_{max} is based on an existing prototype[9,11]. Changes to the reference values would likely change the linear constants in the following analyses, but would not affect the scaling of the parameters.

Using Eq. (9), when *h*, T_{max}, and T_{∞} are held constant, the predicted relationship simplifies to $m \propto L_{max}^{3.5}$. This prediction is shown along with the T-EM model results for 11 Omnimagnets of various sizes of L_{max} in Fig. 2. The magnetic dipole moment *m* is a strong function of Omnimagnet length L_{max} for convectively-cooled Omnimagnets. Permanent magnets typically scale according to L_{max}^3. The additional $L_{max}^{0.5}$ comes from the $q^{0.5}$ in Eq. (8). T-EM model *m* data fit exceptionally well to $L_{max}^{3.5}$. Regression analysis is used to determine a constant $k_L = 1.18 \times 10^5$ A/m$^{1.5}$ such that $m = k_L L_{max}^{3.5}$ closely matches the T-EM data ($r^2 = 0.999$). This equation reveals that small increases in L_{max} can dramatically increase *m* produced by an Omnimagnet and that L_{max} is a critical parameter to consider for Omnimagnet design.

The same procedure is followed to verify the predicted expressions between *m* and temperatures T_{max} and T_{∞}. T_{max} represents the maximum safe temperature that the Omnimagnet can achieve before overheating, and T_{∞} is the temperature of the convection cooling fluid. Simplifying Eq. (9) for constant L_{max} and *h*, the expression becomes $m \propto (T_{max} - T_{\infty})^{0.5}$. This expression is further simplified to $m \propto \Delta T^{0.5}$, where ΔT is the temperature difference $T_{max} - T_{\infty}$. For eight values of T_{max} and twelve values of T_{∞}, *m* produced by an Omnimagnet is calculated via the T-EM model and compared to the predicted expression (Fig. 3). The T-EM data matches $\Delta T^{0.5}$ nearly perfectly, regardless of whether T_{max} or T_{∞} is varied. A regression analysis yields $k_T = 22.1$ A m^2/K$^{0.5}$ ($r^2 = 1.000$). Designing an Omnimagnet to increase ΔT can noticeably increase the produced *m*. This enhancement can be accomplished either by changing materials to increase T_{max} or using a cooled working fluid. Notably, the T-EM model shows that all of the convectively-cooled solenoids or frames operate below T_{max} due to conduction thermal resistances within the device. However, this discrepancy is accounted for using k_T in the scaling model, and the actual temperature distribution is not necessary to accurately predict *m* using the expression.

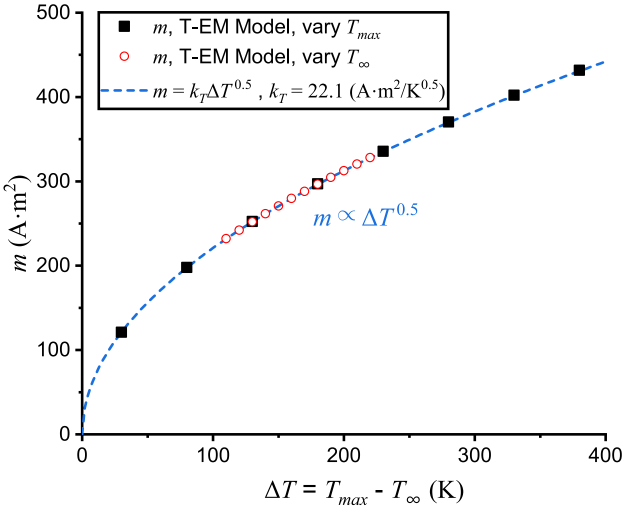

Fig. 3. Verification of predicted expression $m \propto \Delta T^{0.5}$ for a convectively-cooled Omnimagnet. The expression closely matches the T-EM model data for 20 Omnimagnets that vary both T_{max} and T_∞ ($r^2 = 1.000$). Increasing ΔT leads to substantial increases of m produced by an Omnimagnet.

Omnimagnet designs are compared for a wide range of heat transfer coefficients h. The T-EM model data and predicted expression $m \propto h^{0.5}$ do not agree as well as the previous two variables (Fig. 4a). For $h \leq 500$ W/m^2·K, the scaling relation and T-EM model data agree. For $h > 500$ W/m^2·K the T-EM model calculates almost no change in m, while the expression $m \propto h^{0.5}$ continues to increase. This difference is due to an assumption of the scaling analysis: Omnimagnet cooling is completely controlled by convection, and increasing h will always decrease the maximum temperatures. This assumption does not account for any conduction thermal resistance between solenoids. At low h, the ratio of the thermal resistance of convection to the thermal resistance of conduction is much greater than one, and the assumption holds. As h increases, the ratio of convection to conduction thermal resistances decreases. At large h values the ratio becomes less than unity, and the thermal resistance of conduction is non-negligible. This explanation can be readily demonstrated using the temperature profiles inside the Omnimagnet (Fig. 4b). The temperatures of all three solenoids calculated by the T-EM model are shown as a function of h. For $h > 500$ W/m^2·K, increasing h does not appreciably change the solenoid temperatures, because the temperature difference between solenoids is dominated by conduction thermal resistances. The expression $m \propto h^{0.5}$ predicts the heat transfer in this regime quite poorly, but quite well in the convection-limited regime. Thus, the predicted expression is valid only for convection-limited cooling, which in this case is $h \leq 500$ W/m^2·K. This range of h corresponds to free or forced convection using gases or free convection using liquids. A best-fit line is generated via regression for all points $h \leq 500$ W/m^2·K, yielding constant $k_h = 17.8$ A m^3·K$^{0.5}$/W$^{0.5}$ ($r^2 = 0.720$). This finding has interesting implications for Omnimagnet design principles. Increasing h only increases m in convective-limited operation. The relative contribution of convection and conduction thermal resistances should be well understood to maximize m without excessive h.

Predictive thermal-electromagnetic coupling equation for convectively-cooled omnimagnets

Understanding the effects of parametrically varying L_{max}, T_{max}, T_∞, and h on m is useful but mostly intuitive. Newton's Law of Cooling can be used to understand that cooling is increased when, for example, T_{max} increases. Newton's Law of Cooling cannot ascertain the correct scaling exponents, but the enhancement/reduction of cooling is captured. The scaling approach shown in this work goes further: individual expressions can be combined into one expression that directly links the thermal performance to m, the desired electromagnet variable for this application using Eq. (9) and a new variable η_{conv}:

$$m \propto \eta_{conv} = h^{0.5}(T_{max} - T_\infty)^{0.5} L_{max}^{3.5} \quad [\mathrm{W}^{0.5}\mathrm{m}^{2.5}] \tag{10}$$

The value of η_{conv} incorporates the independent scaling of L_{max}, T_{max}, T_∞, and h concurrently. Because $m \propto \eta_{conv}$ the value of η_{conv} can serve as a figure of merit to compare the electromagnetic and thermal performance of different Omnimagnet designs. For two completely different Omnimagnet designs with different η_{conv} values, the higher η_{conv} design will generally produce a larger m as well. In other words, design changes that increase η_{conv} will also increase m, and η_{conv} serves as a figure of merit for estimating the success of an Omnimagnet design. The calculation of η_{conv} also accounts for the relative importance of each parameter. Using η_{conv} allows designers to compare, for example, a 10% increase in L_{max} versus a 50% increase in h, which cannot be done using intuition alone. Newton's Law of Cooling does not give this level of quantitative insight. Designing effective Omnimagnets becomes a simple task of generating multiple designs and comparing the figure of merit η_{conv} for each case.

The ability to compare the absolute m produced by different Omnimagnets is highly desirable. When designing Omnimagnets for new applications it is critical to estimate m produced because the value of m is

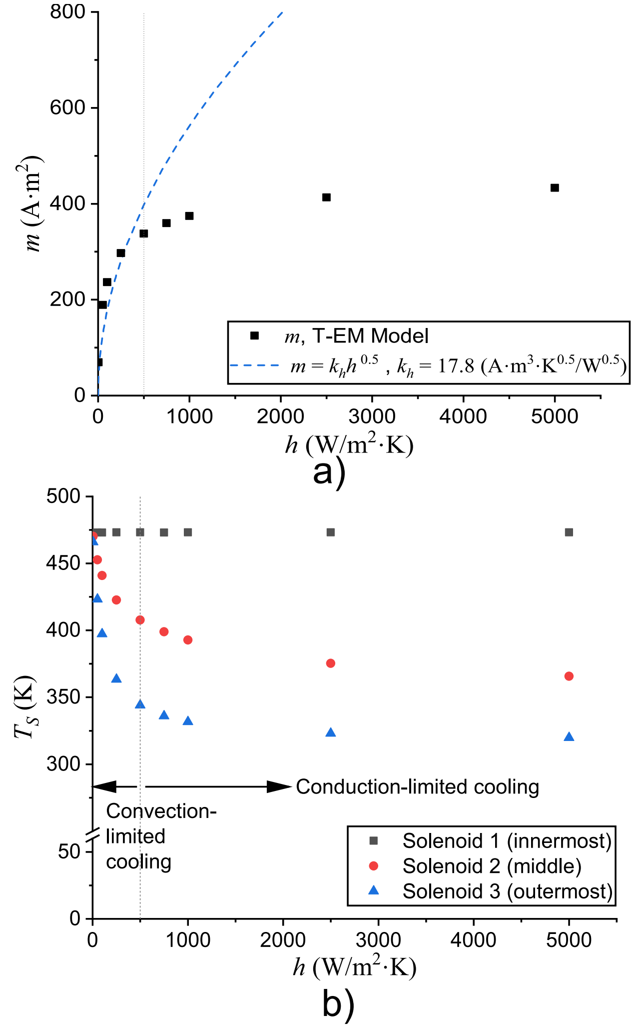

Fig. 4. Verification of predicted expression $m \propto h^{0.5}$ for a convectively-cooled Omnimagnet. (**a**) The expression matches T-EM model data for the convection-limited cooling regime, $h \leq 500$ W/m^2·K, but does not match for conduction-limited cooling. (**b**) Temperature distribution of all three solenoids that demonstrates the shift from convection-limited to conduction-limited cooling.

necessary to calculate the generated forces, torques, and time to complete manipulation tasks. The feasibility of using an Omnimagnet for a given application is unknown until m can be quantitatively estimated. Establishing an equality between η_{conv} and m removes the need for advanced modeling in the feasibility and early design stages.

To establish an equation for calculating m from η_{conv}, a total of 250 Omnimagnet designs are randomly generated across all variables (L_{max}, T_{max}, T_∞, h) within their full ranges as shown in Table 1. The exception is h, which is limited to $h \leq 500$ W/m^2·K according to its valid range. η_{conv} is evaluated for each of the 250 Omnimagnets, and the T-EM model is used to calculate m generated by each case. The coupling variable η_{conv} is then compared to the calculated m (Fig. 5). From visual examination the data are highly linear, indicating a good fit. A line of best fit is obtained via linear regression, which yields $k_{conv} = 530$ A/W$^{0.5}$·m$^{0.5}$ ($r^2 =$ 0.942). The shaded region indicates ±20% error from this coupling equation, which contains nearly all 250 Omnimagnet designs. While precision within ±20% may not be sufficient for finalized designs in biomedical and aerospace applications, it can certainly speed up preliminary system design and suggest operational limits for Omnimagnet systems. All data points that lie outside of the ±20% region are from large Omnimagnets (0.40 m $< L_{max} <$ 0.60 m), and most are near the largest possible size (0.55 m $< L_{max} <$ 0.60 m). These data all use large temperature differences (200 K $< \Delta T <$ 310 K) with moderate to low convective heat transfer coefficients (50 W/m^2·K $< h <$ 200 W/m^2·K). Under these conditions, the convective cooling is underpredicted by the coupling equation, and the predicted m is lower than m from the T-EM model. Despite these niche cases of disagreement, it is clear that for a wide range of h, L_{max}, T_{max}, and T_∞, the dipole moment an Omnimagnet generates can be predicted. The value $k_{conv} = 530$ A/W$^{0.5}$·m$^{0.5}$ is multiplied by η_{conv} in Equation 10 to yield the following equation:

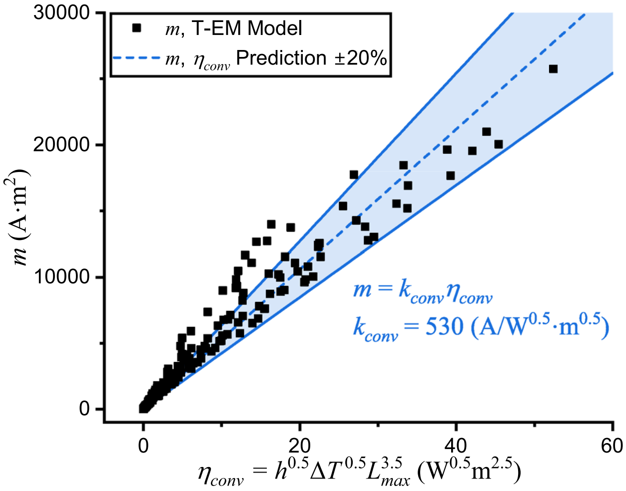

Fig. 5. Thermal-electromagnetic coupling equation to estimate *m* from scaling variable η_{conv}. The best-fit relationship is created by simulating 250 Omnimagnets of random L_{max}, T_{max}, T_∞, and *h*. η_{conv} is able to accurately estimate *m* within ±20% for most cases, and can be used to quantitatively compare completely different Omnimagnet designs.

$$m_{conv} = 530\eta_{conv} = 530h^{0.5}(T_{max} - T_\infty)^{0.5}L_{max}^{3.5} \quad [\mathrm{A}\cdot\mathrm{m}^2] \tag{11}$$

This prediction capability represents a significant advancement in the understanding of Omnimagnet operation. Vastly different Omnimagnet designs can be compared using the figure of merit η_{conv}. *m* generated by each design can be estimated using Eq. (11) to quantitatively predict the performance of convectively-cooled Omnimagnets without the use of advanced simulation techniques. The improvements to *m* are tied directly to the fundamental operation of Omnimagnets, giving further insight into their behavior.

Radiatively-cooled omnimagnet scaling

The above coupling equation only applies for Omnimagnets cooled via convection that are designed to maximize *m*. Other Omnimagnet applications, such as space debris detumbling[2,3], possess radically different design goals and constraints. The strength and flexibility of the figure of merit approach is key, because the same approach can be followed to generate a figure of merit η_{rad} to link thermal and electromagnetic effects for new applications. An Omnimagnet's dipole moment per unit mass, *m*/mass, is critical to maximize for space applications due to the costs associated with launching heavy objects into orbit. These Omnimagnets are conventionally cooled via radiation, which can be modeled using the Stefan-Boltzmann Law[26], $q_{rad} = \varepsilon A_s\sigma(T^4 - T_\infty^4)$, where ε is the average emissivity, A_s is the radiating surface area of solenoid 2, solenoid 3, and frame 4, σ is the Stefan–Boltzmann constant, *T* is the radiating temperature, and T_∞ is the temperature of the surroundings. The surface area can be approximated as $A_s \propto L_{max}^2$, and the radiating temperature as $T \approx T_{max}$. Combining this expression for radiative cooling with Eq. (8) yields the expression for radiatively-cooled Omnimagnets:

$$m \propto \varepsilon^{0.5}\sigma^{0.5}(T_{max}^4 - T_\infty^4)^{0.5}L_{max}^{3.5} \tag{12}$$

Because σ is a constant, it can be combined with the proportionality constant. For space applications $T_\infty \approx 4$ K and is therefore negligible. Finally, the expression should be framed in terms of *m*/mass instead of *m*. Mass can be expressed as density multiplied by volume, which for a cube is $\approx \rho L_{max}^3$. The density of an Omnimagnet is dominated by the ferromagnetic core and is assumed to be constant for most solenoid or frame materials. These simplifications yield the following expression for radiatively-cooled Omnimagnets in space:

$$m/\mathrm{mass} \propto \varepsilon^{0.5}T_{max}^2L_{max}^{0.5} \tag{13}$$

To test this proportionality expression the scaling of each individual component is examined parametrically. The minimum, maximum, and reference values of these variables are shown in Table 2. Reference values are based on a previously constructed prototype[9,11] and previous analysis of radiatively-cooled Omnimagnets[10]. The expressions are compared to *m* values calculated by a coupled thermal-electromagnetic (T-EM) model.

When ε and T_{max} are held constant, Eq. (13) predicts an expression *m*/mass $\propto L_{max}^{0.5}$. Eleven different L_{max} values are used to generate a wide range of Omnimagnet sizes. The *m* value calculated by the T-EM model is then compared to the *m* estimate using $L_{max}^{0.5}$ (Fig. 6). The data from the two methods show tremendous agreement, confirming the predicted expression. Regression analysis is applied to the data to determine a fitting constant $k_L = 12.5$ A m$^{1.5}$/kg ($r^2 = 1.000$). This relationship indicates that even for mass-sensitive applications, it is advantageous to use larger Omnimagnets. The additional *m* produced by large Omnimagnets offsets the extra

Parameter	Minimum	Reference	Maximum
L_{max} [m]	0.025	0.172	0.6
T_{max} [K]	273	473	673
ε_S [–]	0.1	0.6	1
ε_F [–]	0.04	0.04	1

Table 2. Parametric variable ranges for radiatively-cooled omnimagnet.

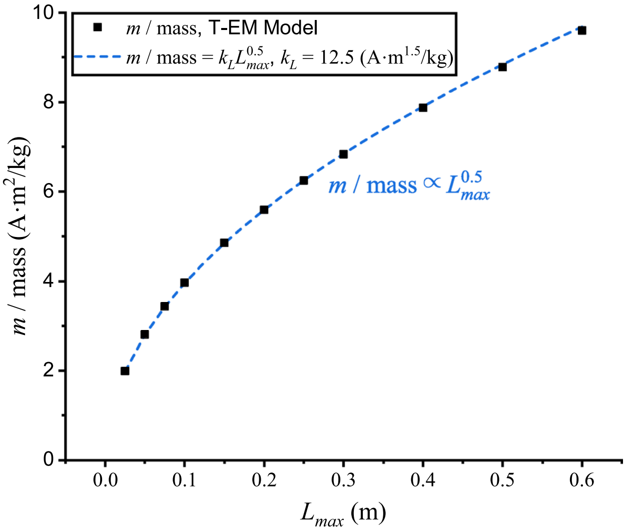

Fig. 6. Verification of predicted expression $m/\text{mass} \propto L_{max}^{0.5}$ for a radiatively-cooled Omnimagnet. The expression closely matches the T-EM model data for 11 Omnimagnets ($r^2 = 1.000$). Increasing L_{max} results in additional mass and additional *m* generation, but the electromagnetic benefits outweigh the mass penalties.

mass that is required. Additionally, the extra surface area enables additional radiative cooling that contributes to the increased *m*.

For constant ε and L_{max}, the predictive expression for maximum allowable Omnimagnet temperature T_{max} is *m*/mass $\propto T_{max}^2$. Notably, this is a departure from the convectively-cooled Omnimagnet, which predicts $m \propto T_{max}^{0.5}$. Maximum temperature T_{max} is varied parametrically to study the effect on *m* and verify the predicted *m*/mass $\propto T_{max}^2$ relationship (Fig. 7). Once again, the expression predicts the electromagnetic performance incredibly well. Regression analysis yields the constant $k_T = 2.28{\times}10^{-5}$ A m^2/kg K^2 (r^2 = 1.000). Intuitively, choosing Omnimagnet materials that increase T_{max} will lead to an increase in *m*.

An Omnimagnet possesses two distinct emissivities: an emissivity of the solenoids, ε_S, and an emissivity of the frames, ε_F. However, for constant L_{max} and T_{max} the proposed expression takes the form $m \propto \varepsilon^{0.5}$, utilizing only a single emissivity. The two separate emissivities are combined into an effective Omnimagnet emissivity based on the fraction of radiating surface area for each component: $\varepsilon_{eff} = A_S\varepsilon_S/A_{total} + A_F\varepsilon_F/A_{total}$. The radiating surface area fractions of the solenoids and frames amount to 83% and 17%, respectively, and $\varepsilon_{eff} = 0.83\varepsilon_S + 0.17\varepsilon_F$. Each of these two emissivities is varied across $0 < \varepsilon \leq 1$ independently while holding the other at the reference value. Both parameters closely match the proposed expression (Fig. 8). Varying ε_S corresponds to a much wider range of ε_{eff} because it is the dominant term. Regression analysis shows that a constant $k_\varepsilon = 7$ A m^2/kg yields an excellent fit ($r^2 = 0.994$).

Predictive thermal-electromagnetic coupling equation for radiatively-cooled omnimagnets

The previous section parametrically validates the expressions of *m*/mass with L_{max}, T_{max}, ε_S, and ε_F. As with the convectively-cooled Omnimagnet case, it is advantageous to combine all separate scaling relationships into a single expression η_{rad}:

$$m/\text{mass} \propto \eta_{rad} = \varepsilon_{eff}^{0.5} T_{max}^2 L_{max}^{0.5} \tag{14}$$

The value of η_{rad} can be used as a figure of merit to compare the relative *m*/mass for different radiatively-cooled Omnimagnet designs. Design changes that increase η_{rad} will tend to increase *m*/mass and vice versa. It is desirable to move from a proportionality expression to an equality between η_{rad} and *m*/mass. This allows designers to predict Omnimagnet perfomance rather than compare across designs. 250 Omnimagnet designs are generated using random values of L_{max}, T_{max}, ε_S, and ε_F between their minimum and maximum values as shown in Table 2. The T-EM model is used to calculate *m*/mass of each Omnimagnet design. This calculated

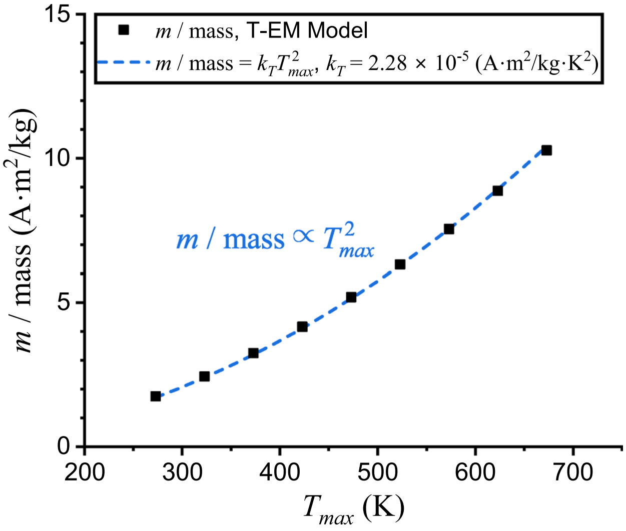

Fig. 7. Verification of predicted expression $m/\text{mass} \propto T^2_{max}$ for a radiatively-cooled Omnimagnet. The expression closely matches the T-EM model data for nine Omnimagnets ($r^2 = 1.000$). Choosing materials that allow T_{max} to increase will increase *m* accordingly.

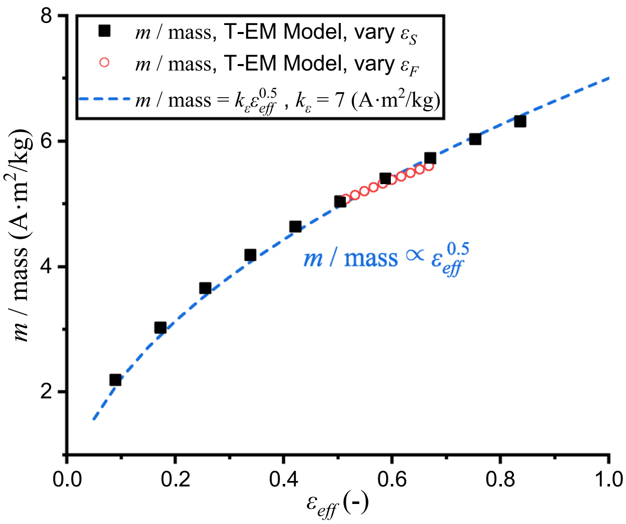

Fig. 8. Verification of predicted expression $m/\text{mass} \propto \varepsilon^{0.5}_{eff}$ for a radiatively-cooled Omnimagnet. The expression closely matches the T-EM model data for 21 Omnimagnets that vary both ε_F and ε_S ($r^2 = 0.994$). Variations in both the frame emissivity and solenoid emissivity are well captured by the scaling analysis.

m/mass is compared to η_{rad} for each case (Fig. 9). Each black data point corresponds to a single randomly generated Omnimagnet design. The data are highly linear, and η_{rad} is able to predict *m* accurately. A linear regression analysis results in a line of best fit using $k_{rad} = 2.40 \times 10^{-5}$ A $\text{m}^{1.5}/\text{K}^2$/kg ($r^2 = 0.942$). The shaded region indicates a deviation of ±10% from the best-fit line and encapsulates nearly all 250 Omnimagnet designs. To predict *m*/mass for radiatively-cooled Omnimagnets, the coupling equation is:

$$m/\text{mass} = (2.40 \times 10^{-5})\varepsilon^{0.5}_{eff} T^2_{max} L^{0.5}_{max} \quad [\text{A} \cdot \text{m}^2] \tag{15}$$

Equation (15) enables engineers and researchers to determine Omnimagnet *m*/mass for any radiatively-cooled design without the need for advanced simulation techniques. Using fundamental Omnimagnet design parameters and Eq. (15) it becomes trivial to determine the performance of any radiatively-cooled Omnimagnet based on *m*/mass metrics. The implementation and design of such Omnimagnets is streamlined using the simple but powerful relations in Eq. (15).

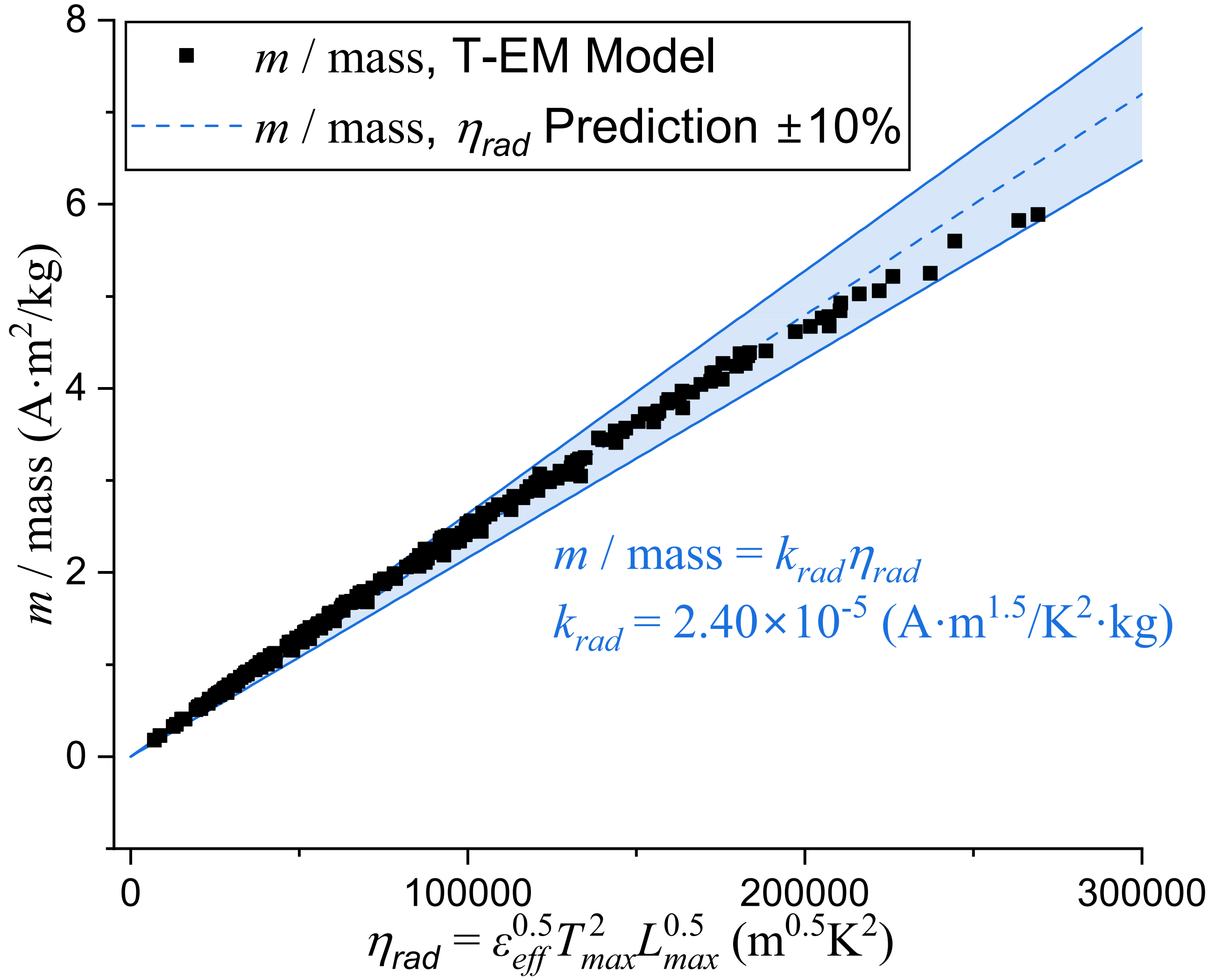

Fig. 9. Coupled thermal-electromagnetic relation to estimate *m*/mass from scaling variable η_{rad}. The best-fit relationship is created by simulating 250 Omnimagnets of random L_{max}, T_{max}, ε_S, and ε_F. η_{rad} is able to accurately estimate *m* within ±10% for all cases, and can be used to quantitatively compare completely different Omnimagnet designs.

Formulating figure of merit expressions for new applications

This section presents the validation of two Omnimagnet expressions that couple thermal and electromagnetic behavior: $m \propto \eta_{conv}$ for convectively-cooled Omnimagnets and *m*/mass $\propto \eta_{rad}$ for radiatively-cooled Omnimagnets. Many other Omnimagnet applications exist, and these applications may use alternative cooling mechanisms or prioritize different electromagnetic quantities. In these cases, Eqs. (11) and (15) are not useful. However, the scaling analysis methodology presented in this work does not assume any application, and Eq. (8) will remain true. The same methodology can be used to generate a new figure of merit expression for any Omnimagnet application. The first step is to determine an expression for the cooling heat transfer rate, q_{out}. The cooling mechanisms could be convection, conduction, radiation, or a combination of two or more. Second, substitute the expression for q_{out} into Eq. (8). Finally, manipulate both sides of the equation to solve for the electromagnetic quantity of interest. This quantity of interest could be *m* or *m*/mass as previously investigated, or focus on an entirely new aspect of Omnimagnet design. As an example, for applications with low power availability or strict power supply requirements, it may be desirable to maximize dipole moment *m* per electrical power input P_{in}. With the understanding that $P_{in} = q_{in} = q_{out}$ at steady-state, the Omnimagnets can be described using:

$$m/P_{in} \propto q_{out}^{-0.5} L_{max}^{2.5} \tag{16}$$

At this point, both convection and radiative cooling can be easily compared via changes to q_{out}. This method gives Omnimagnet designers a straightforward way of comparing designs for applications that have not been previously investigated. If the choice is made to cool these Omnimagnets with radiative cooling, the expression can be rearranged to define η_{power}, a new figure of merit:

$$m/P_{in} \propto \eta_{power} \propto \varepsilon_{eff}^{-0.5} T_{max}^{-2} L_{max}^{1.5} \quad (17)$$

This expression can be used to quickly identify key Omnimagnet design parameters. To maximize m/P_{in} it is clear that T_{max} and ε_{eff} should be minimized, which is counter-intuitive for most radiation applications. Rather than suggesting that radiative heat transfer should be minimized, this expression demonstrates that the Omnimagnet should be run at a lower current and maintained at a lower steady-state temperature, which in turn decreases P_{in}. Increases to L_{max} also benefit m/P_{in}. This case study demonstrates that the methodology in this work can be used to easily generate meaningful relationships between the electromagnetic and thermal effects for Omnimagnets of any application. Engineers considering the use of an Omnimagnet can readily generate these relationships without prior Omnimagnet design experience. Developing such relationships for a wide variety of Omnimagnet applications and cooling mechanisms will expedite the use of Omnimagnets for novel manipulation tasks. Additionally, these expressions provide insight into the fundamental operation of Omnimagnets, bringing attention to the specific design decisions that affect thermal and electromagnetic performance. This methodology ultimately provides a universal framework for Omnimagnet designing across many varied applications.

Conclusion

Current Omnimagnet design processes require advanced modeling capabilities to navigate the non-intuitive thermal-electromagnetic coupling of the device. This work presents a novel method to link the thermal and electromagnetic effects of an Omnimagnet via scaling analysis. This link is critical for understanding how Omnimagnet performance scales with different design parameters. The equations in this work represent a significant step forward in both the understanding of the thermal-electromagnetic coupling and the simplification of the Omnimagnet design process. This approach is adaptable for different cooling mechanisms, such as radiation or convection, as well as different electromagnetic optimizations, such as dipole moment *m* or *m*/mass. Developers are now, for the first time, able to design effective Omnimagnets for any application.

Scaling analysis is used to solve for current density *J* in terms of Joule heating, q_{Joule}, and magnetic dipole moment, *m*. The two expressions are combined to fundamentally link thermal and electromagnetic effects via Eq. (8): $m \propto q_{Joule}^{0.5} L_{max}^{2.5}$. The cooling of an Omnimagnet is equal to the Joule heating at steady-state, meaning $q_{out} = q_{Joule}$. For any cooling mechanism where q_{out} can be defined, Omnimagnet *m* can be tied directly to the thermal management of the system. This is a universal approach that quantitatively links thermal and electromagnetic performance of an Omnimagnet for any application.

The proposed scaling relationships were verified for a convectively-cooled Omnimagnet by comparing the predicted scaling expressions to the results of a previously published coupled thermal-electromagnetic (T-EM) model. All anticipated relationships showed good agreement with the T-EM model. The individual scaling relationships were combined to define a figure of merit η_{conv} that is proportional to *m*: $\eta_{conv} = h^{0.5}(T_{max} - T_\infty)^{0.5} L_{max}^{3.5}$. Using 250 randomly generated Omnimagnet designs, the proportionality was explicitly defined as an equality $m = k_{conv}\eta_{conv}$. The dipole moment produced by most convectively-cooled Omnimagnets can be estimated within ±20% using $m = 530\eta_{conv}$. This equation allows a convectively-cooled Omnimagnet dipole moment *m* to be predicted for many different designs without the use of advanced simulations.

The proposed expressions were also verified for a radiatively-cooled Omnimagnet. Once again, the T-EM model was used for validation. This analysis aimed to understand the link between thermal effects and the dipole moment per mass, *m*/mass. Equation (15), $m/\text{mass} = 2.40 \times 10^{-5}\eta_{rad}$ was shown to estimate *m*/mass within $\pm 10\%$ for all 250 random Omnimagnet designs. This leads to a figure of merit $\eta_{rad} = \varepsilon_{eff}^{0.5} T_{max}^{2} L_{max}^{0.5}$ that quantifies the Omnimagnet performance across many design changes. Although the operation and thermal constraints are fundamentally different than the convectively-cooled case, the same methodology was successfully applied to yield insightful expressions linking thermal and electromagnetic performance.

Equation (8) relates Omnimagnet electromagnetic and thermal performance for any Omnimagnet application and cooling mechanism. For any Omnimagnet where the device cooling rate q_{out} is defined, Equation (8) can be used to generate a figure of merit. As a demonstration, Omnimagnet design was investigated for an entirely new application to maximize *m* per input electrical power, P_{in}, and a new figure of merit η_{power} was established. Regardless of application, Omnimagnet design can now be facilitated by a fundamental understanding of the coupled physics instead of the previous slow, iterative methods. This new method cannot be applied to all Omnimagnet systems: due to the steady-state heat transfer assumption, it is not possible to consider transient changes. Future work to establish a thermal-electromagnetic coupling under transient conditions would be instrumental to the next wave of Omnimagnet design improvements. Additionally, it may be possible to extend this analysis to the design of similar devices, such as the design of permanent magnet electrical machines or helmholtz coils.

Data availability

Data are provided within the manuscript. The raw data required to reproduce these findings are available from the corresponding author upon reasonable request.

Received: 7 March 2025; Accepted: 13 August 2025
Published online: 28 August 2025

References

1. Kessler, D. J. & Cour-Palais, B. G. Collision frequency of artificial satellites: The creation of a debris belt. *J. Geophys. Res. Space Phys.* **83**, 2637–2646. https://doi.org/10.1029/ja083ia06p02637 (1978).
2. Pham, L. N. et al. Dexterous magnetic manipulation of conductive non-magnetic objects. *Nature* **598**, 439–443. https://doi.org/10.1038/s41586-021-03966-6 (2021).
3. Dalton, D. K., Tabor, G. F., Hermans, T. & Abbott, J. J. Attracting conductive nonmagnetic objects with rotating magnetic dipole fields. *IEEE Robot. Autom. Lett.* **7**, 11484–11491. https://doi.org/10.1109/lra.2022.3194878 (2022).
4. Tabor, G. F., Pham, L. N., Abbott, J. J. & Hermans, T. Magnetic manipulation of unknown and complex conductive nonmagnetic objects with application in the remediation of space debris. *Int. J. Robot. Res.* https://doi.org/10.1177/02783649241300167 (2024).
5. Petruska, A. J. & Abbott, J. J. Omnimagnet: An omnidirectional electromagnet for controlled dipole-field generation. *IEEE Trans. Magn.* **50**, 1–10. https://doi.org/10.1109/tmag.2014.2303784 (2014).
6. Bruns, T. L. et al. Magnetically steered robotic insertion of cochlear-implant electrode arrays: system integration and first-in-cadaver results. *IEEE Robot. Autom. Lett.* **5**, 2240–2247. https://doi.org/10.1109/lra.2020.2970978 (2019).
7. Hendricks, C. M. et al. Magnetic steering of robotically inserted lateral-wall cochlear-implant electrode arrays reduces forces on the basilar membrane in vitro. *Otol. Neurotol.* **42**, 1022–1030. https://doi.org/10.1097/mao.0000000000003129 (2021).
8. Pham, L. N. & Abbott, J. J. A soft robot to navigate the lumens of the body using undulatory locomotion generated by a rotating magnetic dipole field. In *2018 IEEE/RSJ International Conference on Intelligent Robots and Systems (IROS)*, 1783–1788. https://doi.org/10.1109/iros.2018.8594247 (2018).
9. Pratt, M., Ameel, T. & Rao, S. R. Modeling of thermal enhancement and scaling analysis for omnidirectional magnetic field generator to actively detumble space debris. *Int. J. Heat Mass Transf.* **241**, https://doi.org/10.1016/j.ijheatmasstransfer.2025.126733 (2025).
10. Pratt, M., Ameel, T. & Rao, S. Coupled thermal-electromagnetic optimization for improved thermal management of omnidirectional magnetic field generators for space applications. *Int. Commun. Heat Mass Transf.* (2025).
11. Esmailie, F., Cavilla, M. S., Abbott, J. J. & Ameel, T. A. Impact of size, structure, and active cooling on the design and control of an omni-directional magnetic field generator: experiments and modeling. *J. Therm. Anal. Calorim.* **147**, 13573–13583. https://doi.org/10.1007/s10973-022-11492-4 (2022).
12. Esmailie, F., Cavilla, M. S., Abbott, J. J. & Ameel, T. A. Thermal model of an omnimagnet for performance assessment and temperature control. *J. Therm. Sci. Eng. Appl.* **13**, https://doi.org/10.1115/1.4049869 (2021). arXiv:2009.05074.
13. Pratt, M., Ameel, T. & Rao, S. Thermal management of omnimagnet for space debris mitigation. In *23rd Intersociety Conference on Thermal and Thermomechanical Phenomena in Electronic Systems*, 1–8. https://doi.org/10.1109/itherm55375.2024.10709577 (2024).
14. Miklavc, A. The solenoid which gives the desired value of magnetic field for the smallest possible volume of conductor. *J. Appl. Phys.* **45**, 1680–1681. https://doi.org/10.1063/1.1663474 (1974).
15. Haignere, E. B. & Potter, W. H. Optimizing the shape and size of a uniform-current-density magnet to maximize the field at constant power. *J. Appl. Phys.* **47**, 1657–1661. https://doi.org/10.1063/1.322788 (1976).
16. Gosselin, L. & Bejan, A. Constructal thermal optimization of an electromagnet. *Int. J. Therm. Sci.* **43**, 331–338. https://doi.org/10.1016/j.ijthermalsci.2003.08.004 (2003).
17. Morgan, P. N. Optimal design and construction of a lightweight minimum-power solenoid magnet. *IEEE Trans. Magn.* **37**, 3814. https://doi.org/10.1109/20.952751 (2001).
18. Huang, Z., Fang, J., Liu, X. & Han, B. Loss calculation and thermal analysis of rotors supported by active magnetic bearings for high-speed permanent-magnet electrical machines. *IEEE Trans. Ind. Electron.* **63**, 2027–2035. https://doi.org/10.1109/tie.2015.2500188 (2016).
19. Dorrell, D. G. Combined thermal and electromagnetic analysis of permanent-magnet and induction machines to aid calculation. *IEEE Trans. Ind. Electron.* **55**, 3566–3574. https://doi.org/10.1109/tie.2008.925311 (2008).
20. Chen, B. *et al.* A study on scaling laws for thermal parameters of permanent magnet synchronous machines. *2021 24th International Conference on Electrical Machines and Systems (ICEMS)* **00**, 35–41. https://doi.org/10.23919/icems52562.2021.9634485 (2021).
21. Pries, J. & Hofmann, H. Magnetic and thermal scaling of electric machines. *Int. J. Veh. Des.* **61**, 219. https://doi.org/10.1504/ijvd.2013.050849 (2013).
22. Madhavan, S. et al. Thermal management analyses of induction motor through the combination of air-cooling and an integrated water-cooling system. *Sci. Rep.* **13**, 10125. https://doi.org/10.1038/s41598-023-36989-2 (2023).
23. Bai, X. et al. Three-dimensional electrochemical-magnetic-thermal coupling model for lithium-ion batteries and its application in battery health monitoring and fault diagnosis. *Sci. Rep.* **14**, 10802. https://doi.org/10.1038/s41598-024-61526-0 (2024).
24. Joule, J. P. On the heat evolved by metallic conductors of electricity, and in the cells of a battery during electrolysis. *Lond. Edinburgh Dublin Philos. Mag. J. Sci.* **19** (1841).
25. Incropera, F. P., Dewitt, D. P., Levine, A. S. & Bergman, T. L. *Fundamentals of Heat and Mass Transfer* 11th edn. (Wiley, Hoboken, 2011).
26. Stefan, J. On the relationship between thermal radiation and temperature. In *Bulletins from the Sessions of the Vienna Academy of Sciences* (1879).

Acknowledgements

This work was supported by the Air Force Research Laboratory, AFWERX, AFRL/RGKB under Contract Nos. FA9453-22-C-A043 and FA864923P1235. This work is part of a collaboration with Rogue Space Systems Corporation.

Author contributions

S.R.R. and T.A. conceptualized and supervised the research and acquired funding. M.P. developed the methodology, performed the simulations, analyzed the data, and drafted the manuscript. All authors reviewed and edited the manuscript.

Declarations

Competing interests

The authors declare no competing interests.

Additional information

Supplementary Information The online version contains supplementary material available at https://doi.org/10.1038/s41598-025-16141-y.

Correspondence and requests for materials should be addressed to S.R.R.